Article

Sex-Specific Effect of Ethanol on Colon Content Lipidome in a Mice Model Using Nontargeted LC/MS

Jayashankar Jayaprakash, Siddabasave Gowda B. Gowda,* Pradeep K. Shukla, Divyavani Gowda, Lipsa Rani Nath, Hitoshi Chiba, Radhakrishna Rao, and Shu-Ping Hui*

Cite This: *ACS Omega* 2024, 9, 16044−16054

Read Online

ACCESS | Metrics & More | Article Recommendations | Supporting Information

ABSTRACT: Consumption of alcohol has widespread effects on the human body. The organs that are most significantly impacted are the liver and digestive system. When alcohol is consumed, it is absorbed in the intestines and processed by the liver. However, excessive alcohol use may affect gut epithelial integrity, microbiome composition, and lipid metabolism. Despite past studies investigating the effect of ethanol on hepatic lipid metabolism, the focus on colonic lipid metabolism has not been well explored. In this study, we investigated the sex-specific effect of ethanol on the colonic content lipidome in a mouse model using nontargeted liquid chromatography−mass spectrometry. Comprehensive lipidome analysis of colonic flush samples was performed using ethanol-fed (EF) and pair-fed (PF) mice of each sex. Partial least-squares discriminant analysis revealed that ethanol altered colonic lipid composition largely in male mice compared with female mice. A significant increase in free fatty acids, ceramides, and hexosylceramides and decreased phosphatidylglycerols (PG) was observed in the EF group compared to the PF group in male mice. Phosphatidylethanolamine (PE) levels were increased significantly in the EF group of both sexes compared to the PF group. The volcanic plot shows that PG (O-15:1/15:0) and PE (O-18:2/15:0) are common markers that are increased in both sexes of the EF group. In addition, decreased fatty acid esters of hydroxy fatty acids (FAHFA) were observed specifically in the EF group of female mice. Overall, a significant variation in the mice colonic content lipidome between the EF and PF groups was observed. Target pathways, such as sphingolipid metabolism in males, FAHFA in females, and PE metabolism in both sexes, were suggested. This study provides new insight into the sex-dependent lipid change associated with alcohol-induced gut-microbiota dysfunction and its potential health impacts.
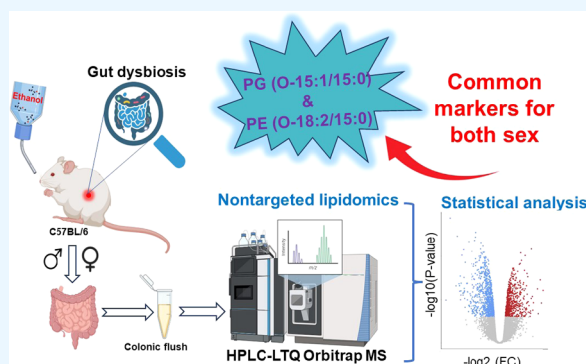
1. INTRODUCTION

Alcohol consumption is a major global cause of mortality, leading to harmful effects on various organs such as the liver, gut, and brain, which results in multisystemic disorders.[1,2] Chronic alcohol use can escalate the risk of alcohol-liver disease (ALD) due to oxidative stress, increased intestinal permeability, and endotoxemia.[3] Extensive research using both animal and human models consistently demonstrates a strong correlation between alcohol consumption and the development of gut dysbiosis.[1,4] The resulting dysbiosis and the direct effects on disruption of intestinal epithelial tight junctions and diffusion of bacterial toxins into intestinal mucosa lead to immune dysfunction and elevated levels of pro-inflammatory cytokines, including tumor necrosis factor (TNF)-α and interleukin (IL)-1β, and further compromise the gut barrier.[5,6] The gut−liver axis plays a pivotal role in mediating alcohol's impact on the digestive system and liver damage, involving the bidirectional transportation of digestive and bacterial products between the gut and liver.[7] The intestinal mucosal barrier function, maintained by tight junction proteins between neighboring enterocytes, serves a crucial role in preserving gut immune function.[8] Alcohol consumption significantly impacts the gut metabolome, leading to substantial alterations in lipid profiles, notably free fatty acids (FFAs), short-chain fatty acids (SCFAs), amino acids, and bile acids.[9] FFAs, derived from the lipolysis of adipose tissue and various cell types, play essential roles as signaling molecule precursors and building blocks for various lipids, including phospholipids (PLs) present in cell membranes.[10,11] Studies have suggested that FFAs, which are integral in ALD, modulate chemokines and cytokines, influencing both pro-inflammatory and inflammation-resolving lipids. Their role extends to shaping functional changes and presenting potential therapeutic targets
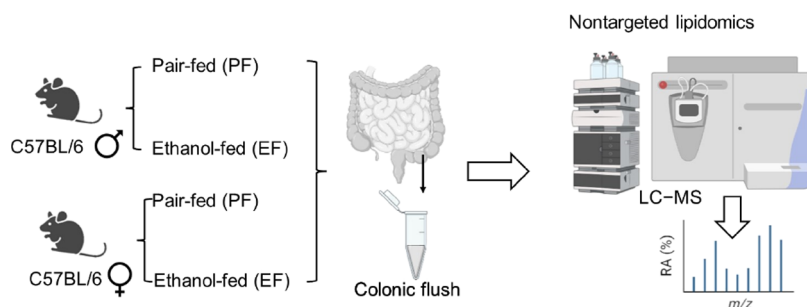
Figure 1. Study design strategy for colon content sample analysis of pair-fed (PF) and ethanol-fed (EF) mice (created with BioRender.com).
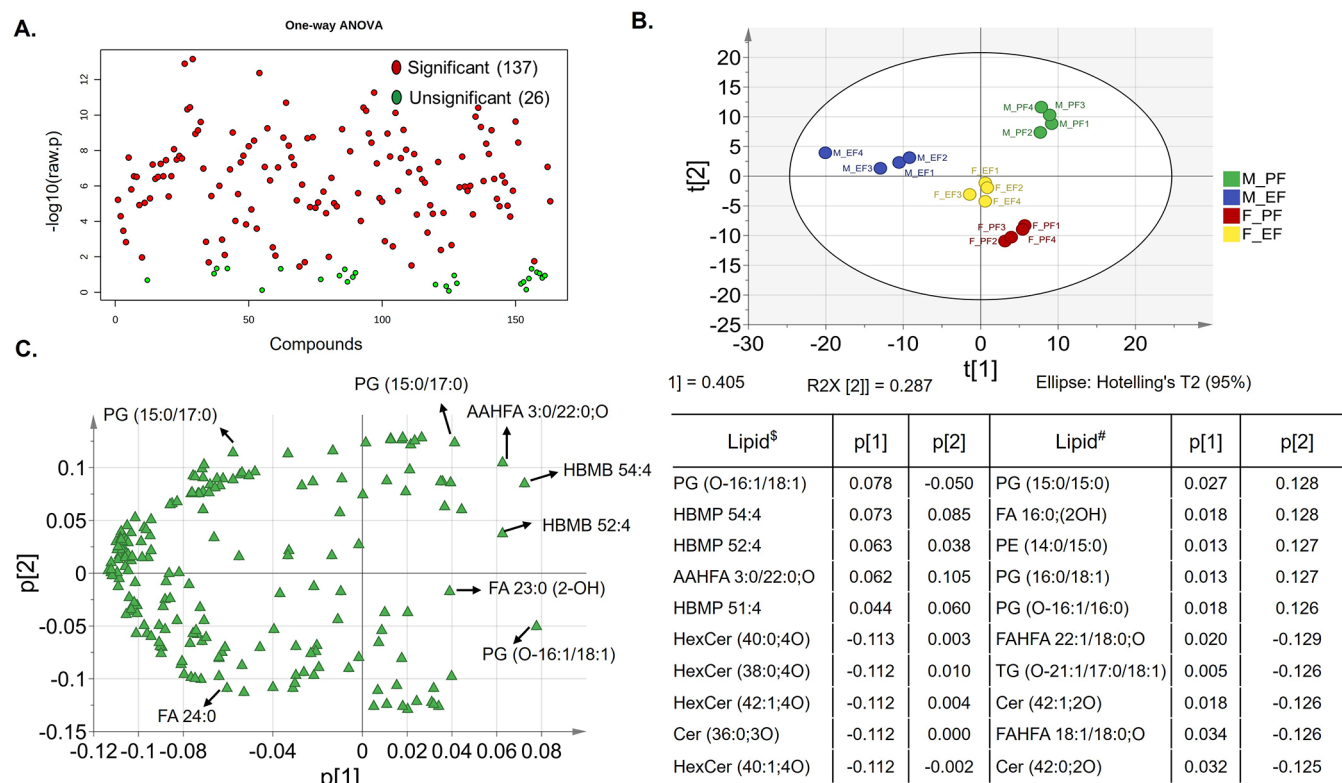
Figure 2. Multivariant analysis of lipid metabolites annotated in PF ($n = 4$) and EF ($n = 4$) samples of both male and female mice. (A) One-way ANOVA analysis of 186 identified lipid molecular species (Tukey's honestly significant difference (HSD) with $p < 0.05$). (B) Principal component analysis (PCA) score plot showing the intrinsic differences between the four cohorts. (C) Loading plot and scores of lipid metabolites from both sexes. The symbols $ and # represent lipids with large positive and negative scores in p[1] and p[2].

for ALD.[12] Conversely, SCFAs, especially butyrate at appropriate concentrations, appear to positively influence gut permeability by potentially reducing intestinal permeability.[13]

Existing studies on lipid metabolism in alcohol-induced gut dysbiosis have certain limitations in understanding the comprehensive relationship between ethanol-induced gut dysbiosis and alterations in host lipid metabolism, particularly in the context of different sexes. Earlier studies have explored specific classes of lipids in the context of ethanol-induced gut dysbiosis using liquid chromatography (LC) coupled to triple quadrupole (QqQ)- and quadrupole time-of-flight (QTOF)/ mass spectrometry (MS) analysis.[14,15] These studies showed that ethanol consumption influences the gut microbiota, leading to alterations in lipid metabolism. However, previous studies on lipid metabolism in ethanol-induced gut dysbiosis are limited to specific lipid classes, and the sex-specific effect of ethanol on gut lipid metabolism remains unclear. In this study, we aimed to systematically investigate the comprehensive

lipidome of the effect of alcohol-induced gut dysbiosis in a mice model of both sexes using high-performance liquid chromatography coupled with linear-ion trap-orbitrap mass spectrometry (HPLC/LTQ-Orbitrap-MS) (Figure 1). To the best of our knowledge, this study represents the first attempt to reveal the sex-specific effect of ethanol on gut lipid metabolism, shedding light on the intricate interplay between alcohol consumption and lipid alterations. This may pave the way for a deeper understanding of the underlying mechanisms and potential therapeutic strategies to address alcohol-related pathologies in a sex-specific context.

2. RESULTS

2.1. Multivariate Analysis and Sex-Specific Lipid Fingerprinting of Ethanol-Fed Mice. Both male and female mice were grouped as pair-fed (PF) and ethanol-fed (EF) mice, and their colonic contents were collected after sacrifice and were subjected to total lipid extraction followed by
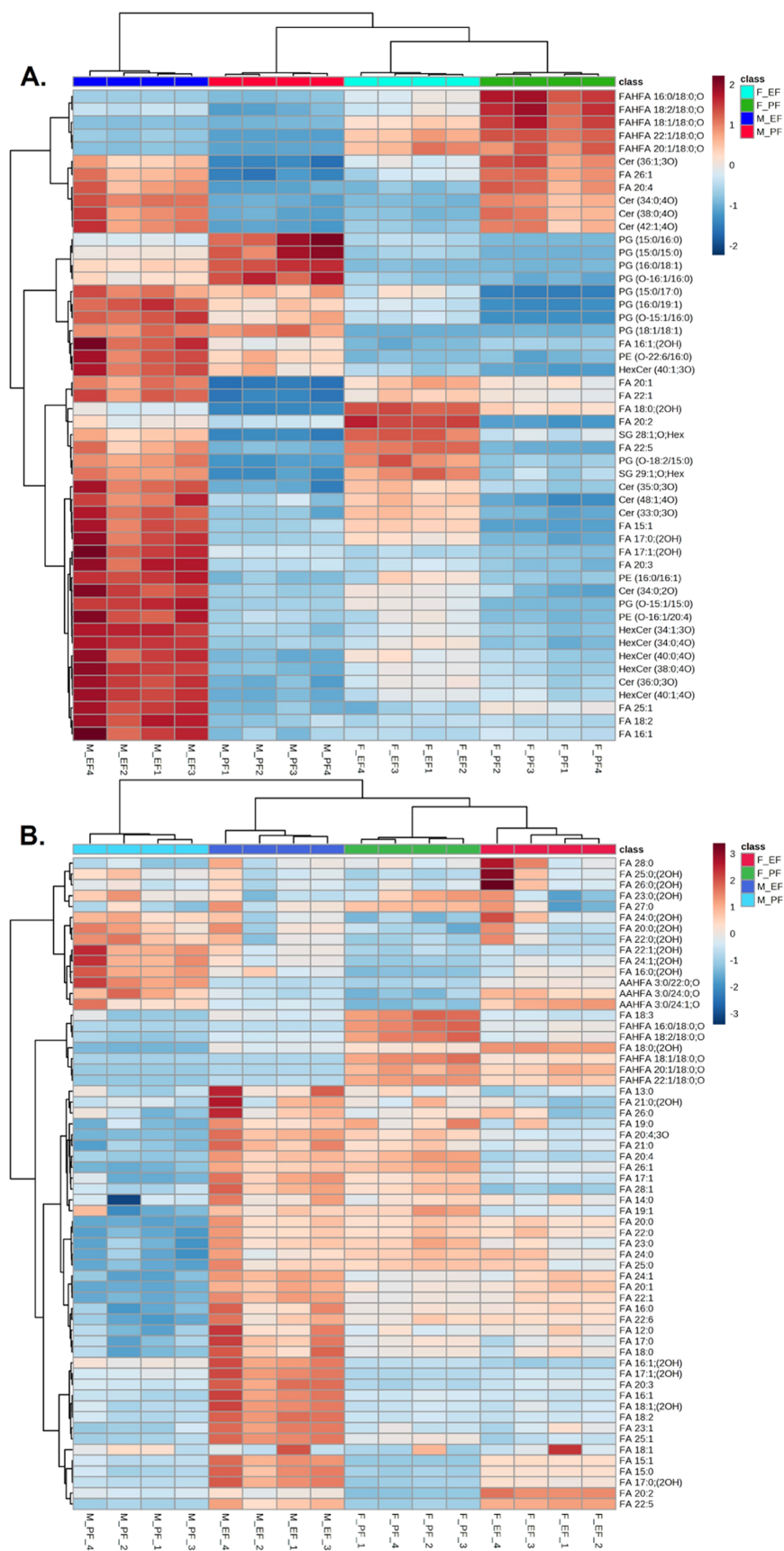
Figure 3. Hierarchical cluster correlation analysis of (A) significantly altered lipids ($p < 0.05$) and (B) fatty acyls observed in both male and female mice of the PF ($n = 4$) and EF ($n = 4$) groups (clustering method: ward, distance measure: Euclidean).
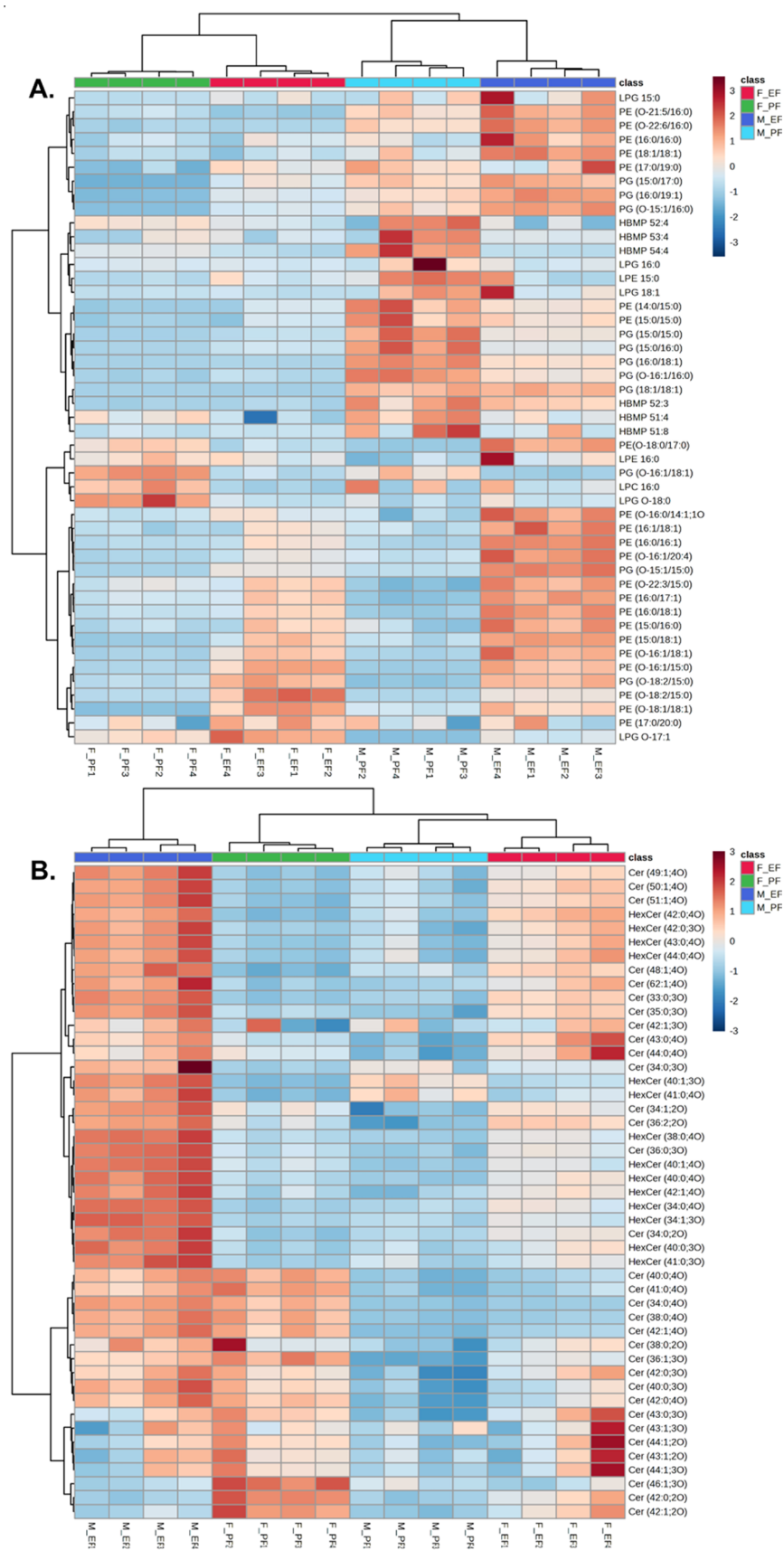
Figure 4. Hierarchical cluster correlation analysis of (A) glycerophospholipids and (B) sphingolipids observed in both male and female mice of the PF ($n = 4$) and EF ($n = 4$) groups (clustering method: ward, distance measure: Euclidean).
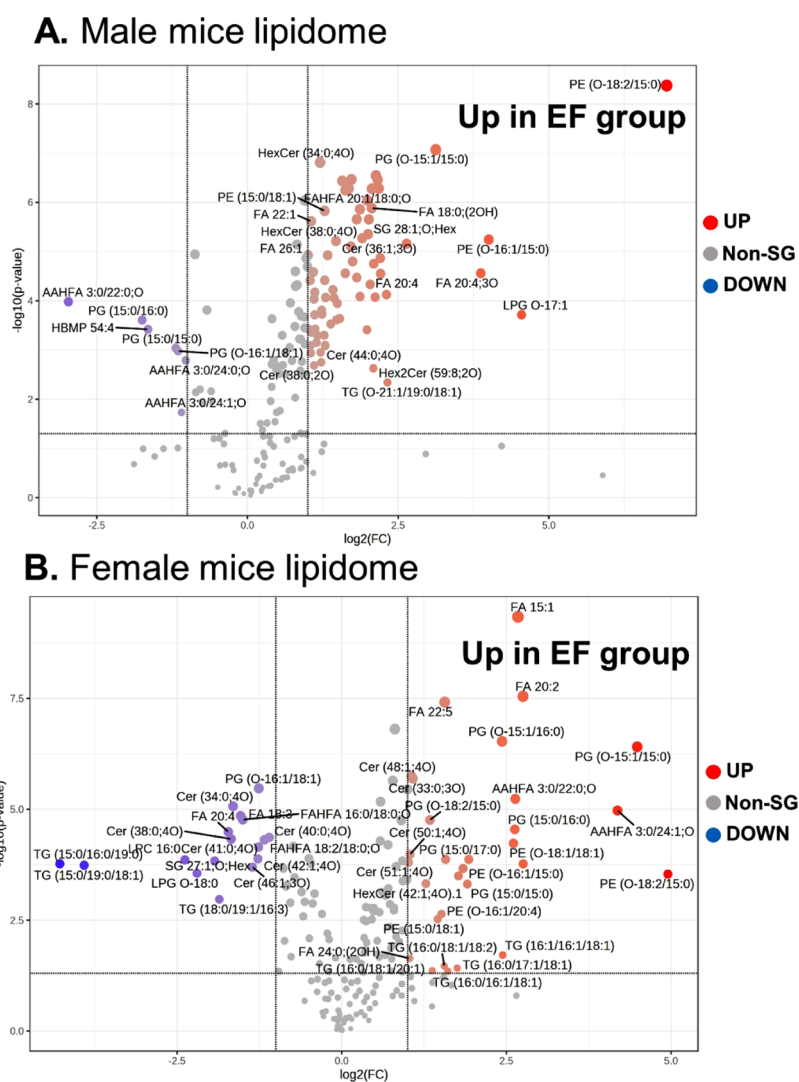
Figure 5. Volcanic plot representing significantly altered lipids (*t*-test, $p < 0.05$) in the colonic flush (A) Male mice in the PF vs EF group ($n = 4$). (B) Female mice in the PF vs EF group ($n = 4$).

nontargeted lipid analysis using HPLC/LTQ-Orbitrap-MS. A comprehensive analysis identified and characterized 186 lipid molecular species based on their exact masses and MS/MS behavior by using MS-DIAL software. The relative concentrations of lipids were calculated based on the amount of added internal standard (IS). The results of one-way analysis of variance (ANOVA) analysis and principal component analysis (PCA) of all of the identified lipid metabolite concentrations are shown in Figure 2. Figure 2A indicates significant vs nonsignificant lipid metabolites based on one-way ANOVA with $p < 0.05$. Out of 186 metabolites, 158 lipid molecular species were statistically significant. The multivariant PCA score plot of the annotated lipids from both male and female PF and EF groups is illustrated in Figure 2B. The two components, component 1 and component 2, accounted for 69.2% of the total variance of models, which was described by 40.5% of component 1.

The analysis revealed two distinct clusters for the male PF and EF groups, indicating clear differentiation among each group lipidome. However, the female PF and EF groups overlapped, indicating fewer lipid compositional differences. The score plot in Figure 2C visually represents the loading plot of the components influencing PCA group differences. The

loading plot indicates the distribution of the variables of importance and the groupings among the samples. Variables with larger positive or negative loading scores in the PCA plot strongly influence the components. Lipid molecular species that largely influence the group separation in the PCA score plot along components 1 and 2 are shown in Figure 2C. The lipids with large positive and large negative loading scores played a significant role in group separation. These results indicate the specific lipids responsible for the observed separation in the two-dimensional PCA plot.

2.2. Hierarchical Cluster Correlation Analysis of Significantly Altered Lipids and Fatty Acyls. The cluster correlation analysis results of the top 50 significantly altered lipids (based on the significance level of *p*-value) between the PF and EF groups of both sexes are shown in Figure 3A. The intense red color indicates the lipids with high concentration, whereas the intense blue color indicates the lipids with low concentration in the respective groups. Compared with female mice, male mice showed drastic changes in colonic lipids due to the effect of alcohol feeding. The lipids shown at the bottom of the heatmap from FA 20:1 to FAHFA 16:0/18:0;O, including several HexCer 34:1;3O, HexCer 34:0;4O, HexCer 40:0;4O, and HexCer 38:0;4O were significantly higher in the
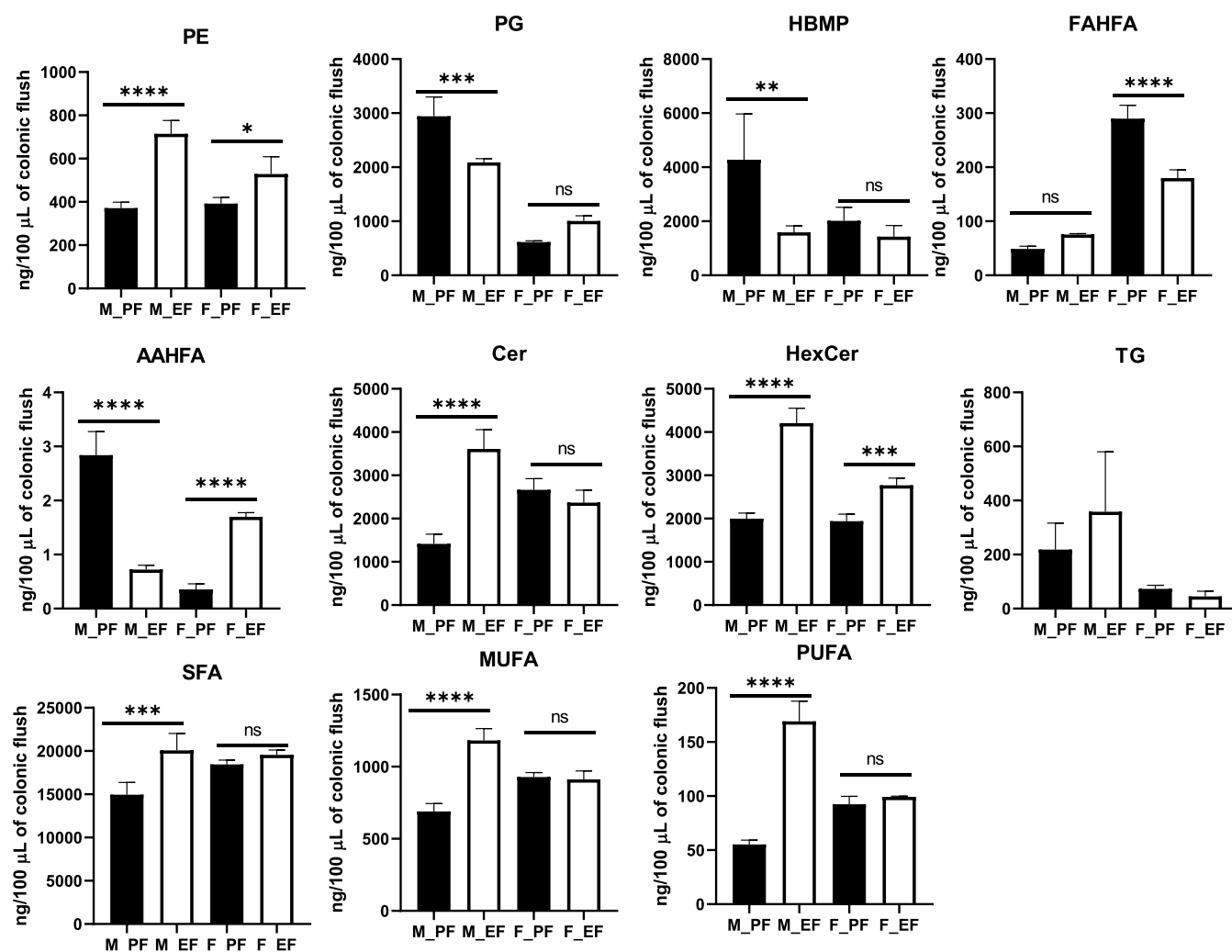
Figure 6. Change in total lipidome at subclass levels in the PF ($n = 4$) and EF ($n = 4$) groups of both sexes. (Ordinary one-way ANOVA, ****$p < 0.0001$, ***$p < 0.001$, **$p < 0.01$, *$p < 0.05$, (ns).)

EF group of male mice than in the PF group. In female mice, lipids such as FA 20:2, FA 22:5, FA 15:1, and ceramides (Cer (35:0;3O), Cer (48:1;4O), Cer (33:0;3O)) are distinctly higher in the EF group than in the PF group. In contrast, FAHFA 16:0/18:0;O, FAHFA 18:2/18:0;O, FAHFA 18:1/18:0;O, and FAHFA 22:1/18:0;O, which are shown at the top of the heatmap are decreased in the EF group of female mice. The cluster correlation analysis results for fatty acyls, including FA, hydroxy fatty acids, fatty acid esters of hydroxy fatty acids (FAHFA), and α acyl hydroxy fatty acid esters (AAHFA) (also known as short-chain fatty acid esters of hydroxy fatty acid (SFAHFA)), are shown in Figure 3B. As mentioned earlier, many fatty acids, including saturated fatty acids (SFAs) (ex: FA 24:0), monounsaturated fatty acids (MUFAs) (ex: FA 20:1), polyunsaturated fatty acids (PUFAs) (ex: FA 22:6), and FA 18:1;(2OH), are increased in the EF group of male mice. In female mice, FA 20:2, FA 22:5, and AAHFA 3:0/24:1;O appeared to be increased in the EF group compared to the PF group.

2.3. Hierarchical Cluster Correlation Analysis of Glycerophospholipids (GPs) and Sphingolipids (SPs). The cluster correlation analysis results of glycerophospholipids (GPs) and sphingolipids (SPs) are visualized as heat maps in Figure 4. In both male and female mice, the GPs, mainly

phosphatidylethanolamine (PE), shown at the bottom of the heatmap of Figure 4A, are higher in the EF group than in the PF group. Other lipid molecular species PG (O-16:1/18:1), lysophosphatidylcholines (LPC 16:0), and lysophosphatidylglycerols (LPG O-18:0) are decreased, whereas PE (O-18:2/15:0), PG (O-18:2/15:0), PE (O-18:1/18:1), PE (O-16:1/15:0), and PE (O-16:1/18:1) are increased in the EF group of female mice specifically compared with the PF group. Similarly, the cluster correlation analysis results of the SPs are listed in Figure 4B. The results indicate that most of the Cer and HexCer are increased in the EF group of male mice compared with the PF group. However, in the case of female mice some specific Cer (i.e., Cer (49:1;4O), Cer (50:1;4O), Cer (51:1;4O)) and HexCer (i.e., HexCer (42:0;4O), HexCer (42:0;3O), HexCer (43:0;4O), HexCer (44:0;4O)) are increased in the EF group. Significant changes in SP levels, specifically in male mice, by the effect of ethanol on gut lipid metabolism suggest that the SP pathway is a potential target for further investigations involving alcohol-induced effects.

2.4. Volcanic Plot Analysis to Identify Sex-Specific Lipid Indicators for the Effect of Alcohol on Gut Metabolism. A volcanic plot represents the graph of $-\log 10(p\text{-value})$ vs $\log 2$ (fold change), describing the significantly and largely altered lipid molecular species.

Volcanic plots for the male and female mice colon content lipidome are shown in Figure 5. The results clearly show significantly upregulated PE (O-18:2/15:0), PG (O-15:1/15:0), and many other lipid molecules indicated in red color (on the right) in the EF group of male mice compared with the PF group (Figure 5A). However, a few lipid molecules such as AAHFA 3:0/22:0;O, PG (15:0/16:0), and other lipids indicated in blue color (on left) are decreased in the colon contents of the EF group. In the case of female mice, FA 15:1, FA 22:5, FA 20:2, PG (O-15:1/16:0), PG (0−15:1/15:0), and many other lipid molecules were increased in the EF group, as described in Figure 5B. In contrast, the lipids PG (O-16:1/18:1), FA 18:3, FA 20:4, and many other lipids annotated in blue color in the below figure are decreased in the EF group. Interestingly, the lipids PG (O-15:1/15:0) and PE (O-18:2/15:0) appear to be a common marker for both sexes as their levels were increased in the colon contents of both male and female mice in the EF group.

2.5. Variation in the Lipidome at the Subclass Level by the Effect of Ethanol Feeding. Figure 6 describes the significantly altered lipidome at subclass levels in both sexes after ethanol feeding. The concentration of each lipid subclass shown in the bar graph is the sum of the individual concentrations of each molecular species of the respective groups. The PE lipids are increased in both male and female mice colon contents of the EF group. However, the rate of increase is higher in male mice than in female mice. PG and hemibismonoacylglycerophosphate (HBMP) were significantly decreased in the EF group of male mice, but no significant changes were observed in female mice. In contrast, the lipids FAHFA were significantly decreased in the EF group of female mice, but no significant changes were observed in the male group. The short-chain fatty acid-derived lipids AAHFA were significantly decreased in the EF group of male mice but showed an opposite trend in female mice. SPs such as Cer were increased in the EF group of male mice but not in female mice. However, HexCer was significantly elevated in the EF group of both sexes compared to that in the PF group. Furthermore, the FA compositions were analyzed at the SFAs, MUFAs, and PUFAs levels. As shown in Figure 6, in all cases, male EF mice had higher concentrations compared with the PF group, whereas female mice did not show any significance in all cases. In summary increased PE, Cer, HexCer, FA, and decreased PG, HBMP are the specific markers for the effect of ethanol on the gut lipid metabolism. In female mice with increased PE, HexCer, and decreased FAHFA, AAHFA appears to be the marker of the ethanol-induced effects on the gut.

3. DISCUSSION

The effect of ethanol on the gut barrier has significant implications for the development and progression of gut dysbiosis. In particular, alcohol consumption is known to disrupt the delicate balance of the gut microbiota composition and increase intestinal mucosal permeability, leading to the translocation of harmful microbial products, such as lipopolysaccharides (LPS), into the blood circulation.[16,17] This phenomenon, often referred to as "leaky gut," has been implicated in the pathogenesis of conditions such as ALD, alcoholic steatohepatitis, and inflammatory bowel disease.[18,19] Lipids play a crucial role in gut metabolism, including the maintenance of the gut barrier integrity. Under normal conditions, the gut mucosa contains a diverse array of lipids, including phospholipids, cholesterol, and various fatty acids.

These lipids contribute to the formation and stability of cell membranes and play a role in maintaining the gut barrier.[20] In this context, dysbiosis induced by ethanol can further disrupt the lipid metabolism in the gut. Studies have shown that ethanol alters the composition of the gut microbiota, leading to increased levels of LPS and other-derived lipids.[21] The extracted ion chromatogram profile, MS, and MS/MS spectrum of representative lipids detected in the colonic flush samples in the present study are shown in the Supporting Information (Figures S1 and S2). The list of identified lipid metabolites and their relative concentrations in the colon contents of PF and EF mice were provided in the Supporting Information (Table S1). Also, the peak area of the internal standards measured in each sample was provided in the Supporting Information (Table S2). Multivariant PCA analysis revealed the group-specific separation in the score plot. To further validate these results, partial least-squares discriminant analysis (PLS-DA) was also performed, and the results are provided in the Supporting Information (Figure S3). PLS-DA analysis revealed a large group separation between PF and EF groups of male mice compared to female mice. Both PCA and PLS-DA results were observed to be similar.

As shown in Figure 3, SFAs [FA 26:0, FA 13:0, FA 21:0 (2OH), FA 12:0, and FA 17:0] and MUFAs [FA 16:1, FA 17:1 (2OH), 18:1 (2OH), and FA 23:1, FA 25:1] were significantly increased in the male EF group compared with the PF group. However, no changes were observed between the PF and EF groups of female mice in SFAs and MUFA levels. Prior research has highlighted the pivotal role of FFA metabolism in the progression development of ALD.[10,22] Several studies show that FFAs have been implicated in the development of alcohol-induced gut dysbiosis, a condition where ethanol consumption leads to imbalances in the gut microbiota composition, potentially contributing to gastrointestinal disorders.[23] In a previous animal study, it was noted that maintaining intestinal levels of FFAs, especially SFAs, has the potential to enhance and maintain the integrity of the intestinal gut barrier.[24] PUFAs such as FA 18:2, FA 20:3, and FA 22:6 were increased in the EF group of the male mice. FA 20:2 and FA 22:5 were increased in the EF group of female mice. Increased MUFAs and PUFAs were also observed in the liver samples of male mice fed with ethanol, and our results in colonic flush are consistent with this finding.[14] In addition, previous study using wild-type (WT) and fat-1 mice exposed to ethanol feeding, total ω-6 PUFAs were significantly higher in the WT-ethanol group and fat-1-ethanol group.[25]

FAHFA are new endogenous lipids with anti-inflammatory and antidiabetic functions.[26] In our results, FAHFA 18:1/18:0;O, FAHFA 20:1/18:0;O, and FAHFA 22:1/18:0;O were decreased, and AAHFA 3:0/24:1;O was increased in the EF group of female mice. AAHFA (3:0/24:0;O) and AAHFA (3:0/22:0;O) were decreased in the EF group of the male mice. AAHFA are also named short-chain fatty acid esters of hydroxy fatty acids (SFAHFA), which were uncovered previously in our laboratory. These lipids tend to be decreased in the colon contents of male rats fed a high-fat diet and increased in the colon contents of male mice infected with influenza virus.[27,28] Furthermore, recent *in-vitro* studies between the mice gut microbiota and FAHFA through spearman correlations analysis showed that *Bacteroides* acidifies could increase the level of FAHFA.[29] Moreover, GPs are the main integral constituents of biological membranes, which play a crucial role in cellular functions. Modulation of GPs is

influenced by alcohol-induced gut dysbiosis.[30] In our results, the total PE levels were significantly increased in the EF group of both male and female mice (Figure 4), but the PG and HBMP levels were decreased specifically in the male EF group. A previous study in male mice fed ethanol for 5 weeks showed decreased PGs in the liver in the EF group compared with controls.[31]

Numerous studies have indicated that SPs possess bioactive properties and play roles in various pathological processes, including cancer, inflammatory disorders, obesity, and neurodegeneration, in both human and animal models.[32,33] In this study, an upregulation of the SPs was detected, especially the total ceramide level in the male EF group, and the total Hexcer level in both male and female EF groups was observed. These results are supported by a previous study that demonstrated Cer upregulation in liver samples of EF mice with dysbiosis.[34] Although no significant differences were observed in the total colonic triacylglycerols (TG level between PF and EF groups of both sexes (Figure S4)). A previous study showed that occludin knockout mice exposed to ethanol exhibited elevated permeability in the colon and heightened triacylglycerol accumulation in the liver, in contrast to wild-type mice.[35] This study benefits the detection of various classes of lipids in both sexes of the PF and EF groups and comprehensive lipid composition analysis. Several limitations need to be addressed in future studies. These include the concentrations reported in this study as semiquantitative, not absolute levels. Further validation experiments with fresh animals in large numbers may be required to consolidate the current findings. The different molecular species of SPs, GPs, and FAs were detected in EF mice samples of both males and females, but the exact mechanism of their metabolism is still unknown.

4. CONCLUSIONS

In conclusion, the flush colon samples of PF and EF mice samples of both sexes were compared and characterized by using lipid profiles to provide new insights into lipid metabolism in alcohol-associated disorders. Relative concentrations of lipid species were observed between PF and EF mice of both males and females. Statistical analysis revealed significant changes in FA and SP levels between the EF and PF groups of male mice. Both male and female EF groups exhibited higher levels of GPs, particularly PG (O-15:1/15:0) and PE (O-18:2/15:0), which emerged as common markers. Female mice in the EF group showed a specific decrease in the levels of fatty acid esters of hydroxy fatty acids (FAHFA), highlighting the importance of this lipid species in alcohol-associated disorders. Overall, the study observed significant variations in the lipidome between mice exposed to the EF and PF diets. This study demonstrated that untargeted lipid profiling using HPLC/LTQ-MS is an effective analytical tool for studying the global lipid profile in mice fed PF and EF diets. This research provides valuable insights into the sex-specific observation of lipid metabolism in alcohol-associated disorders, shedding light on the potential mechanisms underlying these conditions.

5. MATERIALS AND METHODS

5.1. Chemicals and Reagents. LC/MS grade solvents, such as methanol, 2-propanol, and a mobile-phase additive, 1 M aqueous ammonium acetate, were obtained from Wako Pure Chemical Industries, Ltd. (Osaka, Japan). HPLC-grade chloroform was purchased from Sigma-Aldrich (MO). The internal standards EquiSPLASH and oleic acid-d_9 were obtained from Avanti Polar Lipids (Alabaster, AL).

5.2. Animal Samples. Adult (8−10 weeks old) male and female C57BL6 mice bred in our laboratory were used in these studies. The Institutional Animal Care and Use Committee at the University of Tennessee Health Science Center (UTHSC) has approved all of the methods and instructions for the animal studies reported in this work. In our institutional core facility, animals were kept in cages with two animals per cage under 12:12 h light/dark conditions. Before the tests, the animals had full access to regular laboratory food and water.[36]

5.3. Chronic Ethanol Feeding. Mice were fed a Lieber−DiCarli liquid diet (D710260; Dyets Inc., Bethlehem, PA) for 4 weeks with ethanol (0% for 2 days, 1% for 2 days, 2% for 2 days, 4% for 1 week, 5% for 1 week, and 6% for 1 week) or pair-fed isocaloric maltodextrin (BioServ, Flemington, NJ). The diet intakes (mL/g BW/day) were male (PF: 0.68, EF: 0.66) and female (PF: 0.73, EF: 0.72) respectively. Further, the body weights of mice are monitored during the feeding experiments, and the results are provided in Supporting Information Figure S5. At the end of the 4-week feeding period, PF ($n = 4$) and EF ($n = 4$) mice of both sexes were euthanized, and colonic contents were flushed with 3 mL of 0.9% saline. Flushing samples were stored frozen until extraction for lipid analysis.

5.4. Lipid Extraction. Lipid extraction from the flush colon contents of male (PF, EF) and female (PF, EF) mice was performed using the Folch technique, which is a method well-established in our laboratory with minor modifications.[37] In detail, 100 μL of mice colonic flush in PBS was transferred to a 2 mL Eppendorf tube. Subsequently, 100 μL of MeOH and 100 μL of the internal standard (IS) solution were added. The IS solution comprised oleic acid-d_9 (100 μg/mL) and premixed EquiSPLASH Lipidomic (10 μg/mL) in methanol.

After the addition of the IS solution, 400 μL of chloroform was added. The contents were vigorously vortexed at 3500 rpm for 5 min to facilitate the extraction of lipids, followed by centrifugation at 15,000 rpm for 5 min, allowing the separation of the layers. The lower chloroform layer containing the extracted lipids was transferred to a new 2 mL Eppendorf tube. To the residue, 400 μL of chloroform was added again and vortexed for 1 min, followed by centrifugation for 5 min. The upper layer was again transferred to the same new 2 mL Eppendorf tube.[38] Then, it was kept in a centrifuge evaporator at 4 °C for 3 h. Finally, the extract was redissolved in 100 μL of methanol, followed by centrifugation for 10 min at 15,000 rpm, and transferred to LC/MS vials.

5.5. Lipidomic Analysis by HPLC/LTQ-Orbitrap MS. Lipidomic analysis was conducted using an Orbitrap LTQ XL (Thermo-Fisher Scientific Inc., San Jose, CA) coupled with high-performance liquid chromatography (HPLC) based on the LC-20AD UFLC system (Shimadzu Corp., Kyoto, Japan). Lipid separation was achieved using an Atlantis T3 C18 column (2.1 mm × 150 mm, 3 μM, Waters, Milford, MA), with a mobile-phase flow rate of 0.2 mL/min (A: aqueous 10 mM CH_3COONH_4, B: isopropanol, C: methanol) at 40 °C of column temperature throughout the analysis. These LC/MS conditions were consistent with our earlier research.[28] The mobile phase composition was adjusted as follows: 30% B and 35% C from 0 to 1 min, 75% B and 15% C from 1 to 9 min, 82.5% B and 15% C from 9 to 21 min, 95% B and 5% C from 21 to 25 min, 30% B and 35% C from 25 to 26 min, and 30% B

and 35% C from 26 to 30 min. On the other hand, the positive mode analysis used a distinct linear gradient: 30% B and 35% C from 0 to 1 min, 82.5% B and 15% C from 1 to 9 min, followed by a steady state of 95% B and 5% C from 9 to 15 min, 95% B and 5% C from 15 to 25 min. A brief return to 30% B and 35% C was made from 25 to 26 min, and finally, the composition was kept constant at 30% B and 35% C from 26 to 30 min.

We conducted mass spectrometry analysis using an LTQ-Orbitrap mass spectrometer (Thermo-Fisher Scientific Inc., San Jose) in both positive and negative ionization modes. The employed parameters align with those of our previously published reports.[39] For the electrospray ionization (ESI), we set the capillary temperature to 330 °C, the nitrogen-sheath gas flow to 50 units, and the nitrogen auxiliary gas to 20 units. Source and capillary voltages were adjusted to 3 kV and 10 V, respectively, for the negative mode (within scan range: m/z 160−1900) and 4 kV and 25 V, respectively, for the positive mode (within scan range: m/z 150−1950). We performed mass spectrometry analysis in Fourier transform mode with a resolving power of 60,000 to obtain MS^1 spectra. In addition, we acquired low-resolution MS/MS spectra in the ion trap mode at a collision energy of 40 V.[40]

5.6. LC/MS Data Processing and Lipid Quantification.

Data processing used MS-DIAL software version 4.9, which plays a pivotal role in tasks such as data alignment, peak extraction, identification, and peak area integration.[41] The minimum peak height of 1000 amplitude, maximum charged number 2, smoothing level and minimum peak width 3 and 5 scans, mass slice width 0.1 Da, σ window value 0.5, and the identification score cutoff was set to 80%. Further, signal intensity 5 folds greater than the blank was selected with retention time (alignment) and MS^1 tolerance 0.1 min and 0.015 Da, respectively. The lipid identification was confirmed by the retention time behaviors and percentage matching between the reference and experimental MS/MS spectra. The software facilitated a comprehensive analysis and allowed us to accurately identify lipid metabolites. For the relative quantification of lipid molecular species, we followed the guidelines of Lipidomics. This involved calculating the peak area ratios of the identified lipids to the internal standard. To obtain the relative amount of lipids in the samples, these ratios were then multiplied by the concentration of the added internal standard and normalized to the sample volume.

5.7. Statistical Analysis.

The data set used in this study comprised molecular species of lipids in both positive and negative ion modes. Data visualization was performed using Microsoft Excel 2021, and the results were graphically plotted using GraphPad Prism version 8.0.1. Statistical analysis involved One-way ANOVA with Tukey's multiple comparison tests. $p < 0.05$ was performed to identify significant variables. Principal component analysis was conducted using SIMCA 14.1 (Umetrics). The score plot was plotted to assess the degree of similarity between the different groups, and the discriminating features between lipid profiles were identified for each group by showing loading plots (model coefficients vs covariance). One-way ANOVA analysis was conducted using the online platform MetaboAnalyst 5.0 (https://www.metaboanalyst.ca), the following user instructions. All data are presented as the mean $\pm$ the standard deviation (SD).

ASSOCIATED CONTENT

ⓈＩ Supporting Information

The Supporting Information is available free of charge at https://pubs.acs.org/doi/10.1021/acsomega.3c09597.

> Extracted ion chromatograms of lipids (Figure S1); MS and MS/MS spectra of lipids (Figure S2); PLS-DA analysis (Figure S3); correlation analysis heatmap of triacylglycerols (Figure S4); body weight of mice (Figure S5); relative concentration of lipids detected in the colon contents of PF and EF mice (Table S1); and peak area of the internal standards obtained in all four groups of samples (Table S2) (PDF)

AUTHOR INFORMATION

Corresponding Authors

Siddabasave Gowda B. Gowda − *Graduate School of Global Food Resources, Hokkaido University, Sapporo 060-0809, Japan; Faculty of Health Sciences, Hokkaido University, Sapporo 060-0812, Japan;* Ⓞ orcid.org/0000-0002-7972-9982; Email: gowda@gfr.hokudai.ac.jp

Shu-Ping Hui − *Faculty of Health Sciences, Hokkaido University, Sapporo 060-0812, Japan;* Ⓞ orcid.org/0000-0001-7338-076X; Email: keino@hs.hokudai.ac.jp

Authors

Jayashankar Jayaprakash − *Graduate School of Global Food Resources, Hokkaido University, Sapporo 060-0809, Japan*

Pradeep K. Shukla − *Department of Physiology, College of Medicine, University of Tennessee Health Science Center, Memphis, Tennessee 38163, United States*

Divyavani Gowda − *Faculty of Health Sciences, Hokkaido University, Sapporo 060-0812, Japan*

Lipsa Rani Nath − *Graduate School of Global Food Resources, Hokkaido University, Sapporo 060-0809, Japan*

Hitoshi Chiba − *Department of Nutrition, Sapporo University of Health Sciences, Sapporo 007-0894, Japan*

Radhakrishna Rao − *Department of Physiology, College of Medicine, University of Tennessee Health Science Center, Memphis, Tennessee 38163, United States*

Complete contact information is available at:
https://pubs.acs.org/10.1021/acsomega.3c09597

Notes

The authors declare no competing financial interest.

REFERENCES

(1) Rehm, J.; Samokhvalov, A. V.; Shield, K. D. Global Burden of Alcoholic Liver Diseases. *J. Hepatol.* **2013**, *59* (1), 160−168.

(2) Mathurin, P.; Bataller, R. Trends in the Management and Burden of Alcoholic Liver Disease. *J. Hepatol.* **2015**, *62* (1), S38−S46.

(3) Parlesak, A.; Schäfer, C.; Schütz, T.; Bode, J. C.; Bode, C. Increased Intestinal Permeability to Macromolecules and Endotox-

emia in Patients with Chronic Alcohol Abuse in Different Stages of Alcohol-Induced Liver Disease. *J. Hepatol.* **2000**, *32* (5), 742−747.

(4) Litwinowicz, K.; Choroszy, M.; Waszczuk, E. Changes in the Composition of the Human Intestinal Microbiome in Alcohol Use Disorder: A Systematic Review. *Am. J. Drug Alcohol Abuse* **2020**, *46* (1), 4−12.

(5) Bode, C.; Bode, J. C. Effect of Alcohol Consumption on the Gut. *Best Pract. Res., Clin. Gastroenterol.* **2003**, *17* (4), 575−592.

(6) Bala, S.; Marcos, M.; Kodys, K.; Csak, T.; Catalano, D.; Mandrekar, P.; Szabo, G. Up-Regulation of MicroRNA-155 in Macrophages Contributes to Increased Tumor Necrosis Factor {alpha} (TNF{alpha}) Production via Increased MRNA Half-Life in Alcoholic Liver Disease. *J. Biol. Chem.* **2011**, *286* (2), 1436−1444.

(7) Zima, T.; Kalousová, M. Oxidative Stress and Signal Transduction Pathways in Alcoholic Liver Disease. *Alcohol: Clin. Exp. Res.* **2005**, *29* (11 Suppl), 110S−115S.

(8) Suzuki, T. Regulation of Intestinal Epithelial Permeability by Tight Junctions. *Cell. Mol. Life Sci.* **2013**, *70* (4), 631−659.

(9) Silva, Y. P.; Bernardi, A.; Frozza, R. L. The Role of Short-Chain Fatty Acids From Gut Microbiota in Gut-Brain Communication. *Front. Endocrinol.* **2020**, *11*, No. 25, DOI: 10.3389/fendo.2020.00025.

(10) Jeon, S.; Carr, R. Alcohol Effects on Hepatic Lipid Metabolism. *J. Lipid Res.* **2020**, *61* (4), 470−479.

(11) van Meer, G.; Voelker, D. R.; Feigenson, G. W. Membrane Lipids: Where They Are and How They Behave. *Nat. Rev. Mol. Cell Biol.* **2008**, *9* (2), 112−124.

(12) Voutilainen, T.; Kärkkäinen, O. Changes in the Human Metabolome Associated With Alcohol Use: A Review. *Alcohol Alcohol.* **2019**, *54* (3), 225−234.

(13) Binienda, A.; Twardowska, A.; Makaro, A.; Salaga, M. Dietary Carbohydrates and Lipids in the Pathogenesis of Leaky Gut Syndrome: An Overview. *Int. J. Mol. Sci.* **2020**, *21* (21), No. 8368, DOI: 10.3390/ijms21218368.

(14) Fang, C.; Zhou, Q.; Liu, Q.; Jia, W.; Xu, Y. Crosstalk between Gut Microbiota and Host Lipid Metabolism in a Mouse Model of Alcoholic Liver Injury by Chronic Baijiu or Ethanol Feeding. *Food Funct.* **2022**, *13* (2), 596−608.

(15) Yasuda, S.; Okahashi, N.; Tsugawa, H.; Ogata, Y.; Ikeda, K.; Suda, W.; Arai, H.; Hattori, M.; Arita, M. Elucidation of Gut Microbiota-Associated Lipids Using LC-MS/MS and 16S RRNA Sequence Analyses. *iScience* **2020**, *23* (12), No. 101841.

(16) Bishehsari, F.; Engen, P. A.; Preite, N. Z.; Tuncil, Y. E.; Naqib, A.; Shaikh, M.; Rossi, M.; Wilber, S.; Green, S. J.; Hamaker, B. R.; Khazaie, K.; Voigt, R. M.; Forsyth, C. B.; Keshavarzian, A. Dietary Fiber Treatment Corrects the Composition of Gut Microbiota, Promotes SCFA Production, and Suppresses Colon Carcinogenesis. *Genes* **2018**, *9* (2), No. 102, DOI: 10.3390/genes9020102.

(17) Mutlu, E. A.; Gillevet, P. M.; Rangwala, H.; Sikaroodi, M.; Naqvi, A.; Engen, P. A.; Kwasny, M.; Lau, C. K.; Keshavarzian, A. Colonic Microbiome Is Altered in Alcoholism. *Am. J. Physiol.: Gastrointest. Liver Physiol.* **2012**, *302* (9), G966−G978.

(18) Mendes, B. G.; Schnabl, B. From Intestinal Dysbiosis to Alcohol-Associated Liver Disease. *Clin. Mol. Hepatol.* **2020**, *26* (4), 595−605.

(19) Salim, S. Y.; Söderholm, J. D. Importance of Disrupted Intestinal Barrier in Inflammatory Bowel Diseases. *Inflammatory Bowel Dis.* **2011**, *17* (1), 362−381.

(20) Cani, P. D.; Bibiloni, R.; Knauf, C.; Waget, A.; Neyrinck, A. M.; Delzenne, N. M.; Burcelin, R. Changes in Gut Microbiota Control Metabolic Endotoxemia-Induced Inflammation in High-Fat Diet-Induced Obesity and Diabetes in Mice. *Diabetes* **2008**, *57* (6), 1470−1481.

(21) Yan, A. W.; Fouts, D. E.; Brandl, J.; Stärkel, P.; Torralba, M.; Schott, E.; Tsukamoto, H.; Nelson, K. E.; Brenner, D. A.; Schnabl, B. Enteric Dysbiosis Associated with a Mouse Model of Alcoholic Liver Disease. *Hepatology* **2011**, *53* (1), 96−105.

(22) Hwang, S.; Gao, B. How Does Your Fat Affect Your Liver When You Drink? *J. Clin. Invest.* **2019**, *129* (6), 2181−2183.

(23) Hartmann, P.; Seebauer, C. T.; Schnabl, B. Alcoholic Liver Disease: The Gut Microbiome and Liver Cross Talk. *Alcohol.: Clin. Exp. Res.* **2015**, *39* (5), 763−775.

(24) Chen, P.; Torralba, M.; Tan, J.; Embree, M.; Zengler, K.; Stärkel, P.; van Pijkeren, J.-P.; DePew, J.; Loomba, R.; Ho, S. B.; Bajaj, J. S.; Mutlu, E. A.; Keshavarzian, A.; Tsukamoto, H.; Nelson, K. E.; Fouts, D. E.; Schnabl, B. Supplementation of Saturated Long-Chain Fatty Acids Maintains Intestinal Eubiosis and Reduces Ethanol-Induced Liver Injury in Mice. *Gastroenterology* **2015**, *148* (1), 203.e16−214.e16.

(25) Warner, D. R.; Warner, J. B.; Hardesty, J. E.; Song, Y. L.; King, T. N.; Kang, J. X.; Chen, C.-Y.; Xie, S.; Yuan, F.; Prodhan, M. A. I.; Ma, X.; Zhang, X.; Rouchka, E. C.; Maddipati, K. R.; Whitlock, J.; Li, E. C.; Wang, G. P.; McClain, C. J.; Kirpich, I. A. Decreased ω-6:ω-3 PUFA Ratio Attenuates Ethanol-Induced Alterations in Intestinal Homeostasis, Microbiota, and Liver Injury. *J. Lipid Res.* **2019**, *60* (12), 2034−2049.

(26) Yore, M. M.; Syed, I.; Moraes-Vieira, P. M.; Zhang, T.; Herman, M. A.; Homan, E. A.; Patel, R. T.; Lee, J.; Chen, S.; Peroni, O. D.; Dhaneshwar, A. S.; Hammarstedt, A.; Smith, U.; McGraw, T. E.; Saghatelian, A.; Kahn, B. B. Discovery of a Class of Endogenous Mammalian Lipids with Anti-Diabetic and Anti-Inflammatory Effects. *Cell* **2014**, *159* (2), 318−332.

(27) Gowda, S. G. B.; Liang, C.; Gowda, D.; Hou, F.; Kawakami, K.; Fukiya, S.; Yokota, A.; Chiba, H.; Hui, S. Identification of Short-chain Fatty Acid Esters of Hydroxy Fatty Acids (SFAHFAs) in a Murine Model by Nontargeted Analysis Using Ultra-high-performance Liquid Chromatography/Linear Ion Trap Quadrupole-Orbitrap Mass Spectrometry. *Rapid Commun. Mass Spectrom.* **2020**, *34* (17), No. e8831, DOI: 10.1002/rcm.8831.

(28) Gowda, S. G. B.; Gowda, D.; Ohno, M.; Liang, C.; Chiba, H.; Hui, S.-P. Detection and Structural Characterization of SFAHFA Homologous Series in Mouse Colon Contents by LTQ-Orbitrap-MS and Their Implication in Influenza Virus Infection. *J. Am. Soc. Mass Spectrom.* **2021**, *32* (8), 2196−2205.

(29) Yan, S.; Zhu, Y.; Li, L.; Qin, S.; Yuan, J.; Chang, X.; Hu, S. Alginate Oligosaccharide Ameliorates Azithromycin-Induced Gut Microbiota Disorder via Bacteroides Acidifaciens-FAHFAs and Bacteroides-TCA Cycle Axes. *Food Funct.* **2023**, *14* (1), 427−444.

(30) Wang, X.; Li, L.; Bian, C.; Bai, M.; Yu, H.; Gao, H.; Zhao, J.; Zhang, C.; Zhao, R. Alterations and Correlations of Gut Microbiota, Fecal, and Serum Metabolome Characteristics in a Rat Model of Alcohol Use Disorder. *Front. Microbiol.* **2023**, *13*, No. 1068825.

(31) Koelmel, J. P.; Tan, W. Y.; Li, Y.; Bowden, J. A.; Ahmadireskety, A.; Patt, A. C.; Orlicky, D. J.; Mathé, E.; Kroeger, N. M.; Thompson, D. C.; Cochran, J. A.; Golla, J. P.; Kandyliari, A.; Chen, Y.; Charkoftaki, G.; Guingab-Cagmat, J. D.; Tsugawa, H.; Arora, A.; Veselkov, K.; Kato, S.; Otoki, Y.; Nakagawa, K.; Yost, R. A.; Garrett, T. J.; Vasiliou, V. Lipidomics and Redox Lipidomics Indicate Early Stage Alcohol-Induced Liver Damage. *Hepatol. Commun.* **2022**, *6* (3), 513−525.

(32) Gomez-Larrauri, A.; Presa, N.; Dominguez-Herrera, A.; Ouro, A.; Trueba, M.; Gomez-Muñoz, A. Role of Bioactive Sphingolipids in Physiology and Pathology. *Essays Biochem.* **2020**, *64* (3), 579−589.

(33) Alaamery, M.; Albesher, N.; Aljawini, N.; Alsuwailm, M.; Massadeh, S.; Wheeler, M. A.; Chao, C.-C.; Quintana, F. J. Role of Sphingolipid Metabolism in Neurodegeneration. *J. Neurochem.* **2021**, *158* (1), 25−35.

(34) Clugston, R. D.; Jiang, H.; Lee, M. X.; Piantedosi, R.; Yuen, J. J.; Ramakrishnan, R.; Lewis, M. J.; Gottesman, M. E.; Huang, L.-S.; Goldberg, I. J.; Berk, P. D.; Blaner, W. S. Altered Hepatic Lipid Metabolism in C57BL/6 Mice Fed Alcohol: A Targeted Lipidomic and Gene Expression Study. *J. Lipid Res.* **2011**, *52* (11), 2021−2031.

(35) Ballway, J. W.; Song, B.-J. Translational Approaches with Antioxidant Phytochemicals against Alcohol-Mediated Oxidative Stress, Gut Dysbiosis, Intestinal Barrier Dysfunction, and Fatty Liver Disease. *Antioxidants* **2021**, *10* (3), No. 384, DOI: 10.3390/antiox10030384.

(36) Meena, A. S.; Shukla, P. K.; Rao, R.; Canelas, C.; Pierre, J. F.; Rao, R. TRPV6 Deficiency Attenuates Stress and Corticosterone-Mediated Exacerbation of Alcohol-Induced Gut Barrier Dysfunction and Systemic Inflammation. *Front. Immunol.* **2023**, *14*, No. 1093584.

(37) Gowda, S. G. B.; Gowda, D.; Hou, F.; Chiba, H.; Parcha, V.; Arora, P.; Halade, G. V.; Hui, S.-P. Temporal Lipid Profiling in the Progression from Acute to Chronic Heart Failure in Mice and Ischemic Human Hearts. *Atherosclerosis* **2022**, *363*, 30−41.

(38) Gowda, S. G. B.; Gao, Z.-J.; Chen, Z.; Abe, T.; Hori, S.; Fukiya, S.; Ishizuka, S.; Yokota, A.; Chiba, H.; Hui, S.-P. Untargeted Lipidomic Analysis of Plasma from High-Fat Diet-Induced Obese Rats Using UHPLC-Linear Trap Quadrupole-Orbitrap MS. *Anal. Sci.* **2020**, *36* (7), 821−828.

(39) Gowda, S. G. B.; Minami, Y.; Gowda, D.; Chiba, H.; Hui, S.-P. Detection and Characterization of Lipids in Eleven Species of Fish by Non-Targeted Liquid Chromatography/Mass Spectrometry. *Food Chem.* **2022**, *393*, No. 133402.

(40) Gowda, S. G. B.; Sasaki, Y.; Hasegawa, E.; Chiba, H.; Hui, S.-P. Lipid Fingerprinting of Yellow Mealworm *Tenebrio molitor* by Untargeted Liquid Chromatography-Mass Spectrometry. *J. Insects Food Feed* **2022**, *8* (2), 157−168.

(41) Gowda, S. G. B.; Yifan, C.; Gowda, D.; Tsuboi, Y.; Chiba, H.; Hui, S.-P. Analysis of Antioxidant Lipids in Five Species of Dietary Seaweeds by Liquid Chromatography/Mass Spectrometry. *Antioxidants* **2022**, *11* (8), No. 1538, DOI: 10.3390/antiox11081538.